Capacity reduction caused by air intake at wastewater pumping stations

Christof L. Lubbers[*, **], François H.L.R. Clemens***
** WL | Delft Hydraulics, P.O. Box 177, 2600 MH Delft, the Netherlands. Christof.Lubbers@WLDelft.nl*
*** Section of Sanitary Engineering, Faculty of Civil Engineering and Geosciences, Delft University of Technology P.O. Box 5048, 2600 GA Delft, the Netherlands. F.h.l.r.clemens@citg.tudelft.nl*

Abstract
In the Netherlands, wastewater is normally collected in combined sewer system and pumped to the WWTP through pressure mains. These pressure mains are a part of the system that did not receive much attention lately with respect to monitoring of performance and maintenance. A recent inventory showed that about half of the pressure mains suffer from increased pressure loss for no obvious reason. Reduction of the systems nominal capacity may be caused by many things, such as increased wall roughness, scaling and occurrence of free gas in the pipeline. Free gas may be caused by degassing of dissolved gas, but also by air entrainment at the pump's inlet or at air valves.

Experiments have been conducted with DN200 pipes to investigate the influence of entrapped gas on the head loss of wastewater systems on the transport phenomena of gas. The critical flow velocity to transport gas in downward inclined pipes is investigated as a function of the pipe angle and water flow rate. This paper describes the first results of the experiments.

Keywords: wastewater transport mains, capacity reduction, gas-liquid mixture experiments, phenomenon description.

1 INTRODUCTION

The hydraulic capacity of pressure mains does change during its operational life because of scaling, the occurrence of air/gas pockets, wear of pumps etc. In practical cases it is no trivial task to identify the cause of capacity loss in the first place. To find a sound solution for a 'problematic' pressure main is in many cases even more difficult since in a significant number of cases a basic design problem of the pumping station seems to be the cause. Free gas in pressurised pipelines/mains can significantly reduce the flow capacity. When the capacity of wastewater pressure mains fails to be in line with the design value, undesirable spills or efficiency loss may be the result.

Delft Hydraulics and Delft University of Technology started an extensive research programme in 2003 into these processes. The objectives of this programme are:
- Developing a method to diagnose the cause of capacity loss of a pressure main.
- Get insight in the processes and main parameters influencing scaling.
- A quantitative understanding of the processes involved in the dynamics of air/gas pockets in pressure mains
- Obtain a better code of design practice in terms of avoiding scaling and the occurrence of persistent air/gas pockets in pressure mains.

In this paper only the third objective mentioned is addressed, discussing preliminary results only.

At present, only little is known about the influence of the wastewater properties on the transport of air/gas pockets in pressure mains when compared to clean water. The generally used equations for critical velocity of gas transport (e.g. Kent (1952), Wisner (1975), Walski (1994) are based on experiments carried out with clean water and small pipe diameters. It is likely that for wastewater with its divergent properties compared to clean water these equations are not valid. Figure 1 shows the differences in critical velocity given in literature. Some preliminary results of the Delft experiments are indicated also.

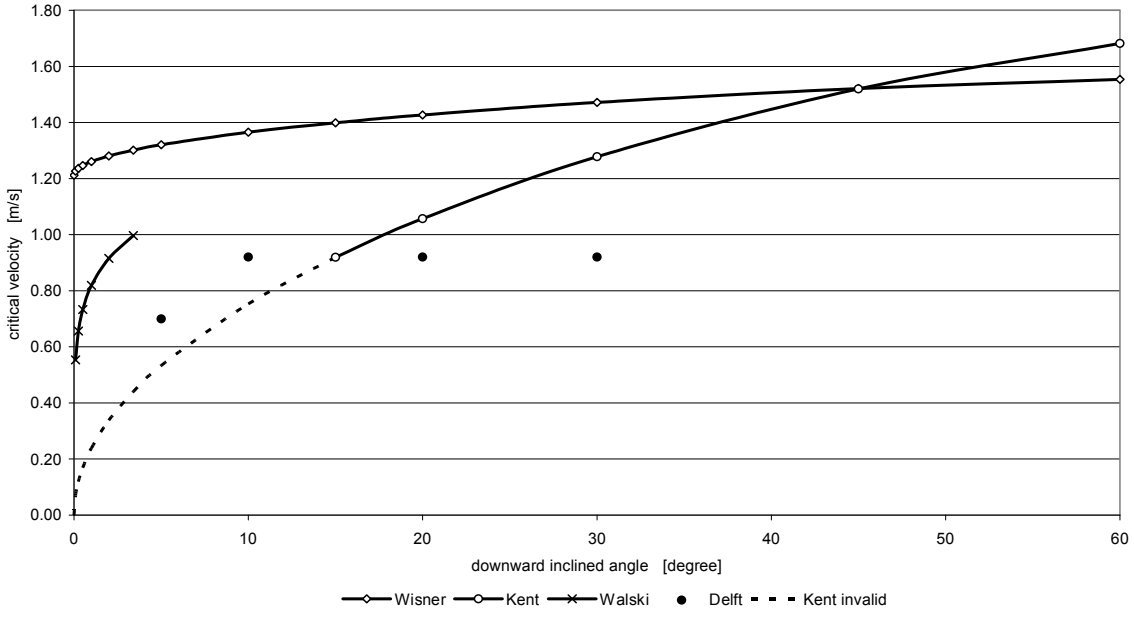

Figure 1: Critical velocity as a function of pipe angle.

2 AIR INTODUCTION IN RELATION TO PUMPING STATION DESIGN

Free gas can be introduced to the system in many ways, such as biogas that dissolves at low pressure points along the pipeline and malfunctioning (air) valves that are located at locations below the hydraulic grade line. Some design features of wastewater pumping stations may cause introduction of air into the system. A few possible design flaws are discussed hereafter.

2.1 Sewer supply pipe

The sewer supply pipe to the suction reservoir is often located purposefully above the switch-on level, to drain the sewer as much as possible. The downside to this design is that the sewer water always enters the reservoir as a plunging jet, entraining large amounts of air into the reservoir water. A lot of the sewer reservoirs have a compact, rounded off design in order to keep solids into suspension and to prevent the reservoir from being clogged. This design results in a short residence time of the wastewater and thus causing increased risk of transporting the air bubbles further into the system. Figure 2 left shows an example of a standard pumping station. The bottom of the sewer water supply pipe is located at the water level at which the pump is switched on (MAX WL). Figure 2 right shows the top view of the reservoir. The sewer supply flow plunges in between the two pumps, entraining air to the pump suction area.

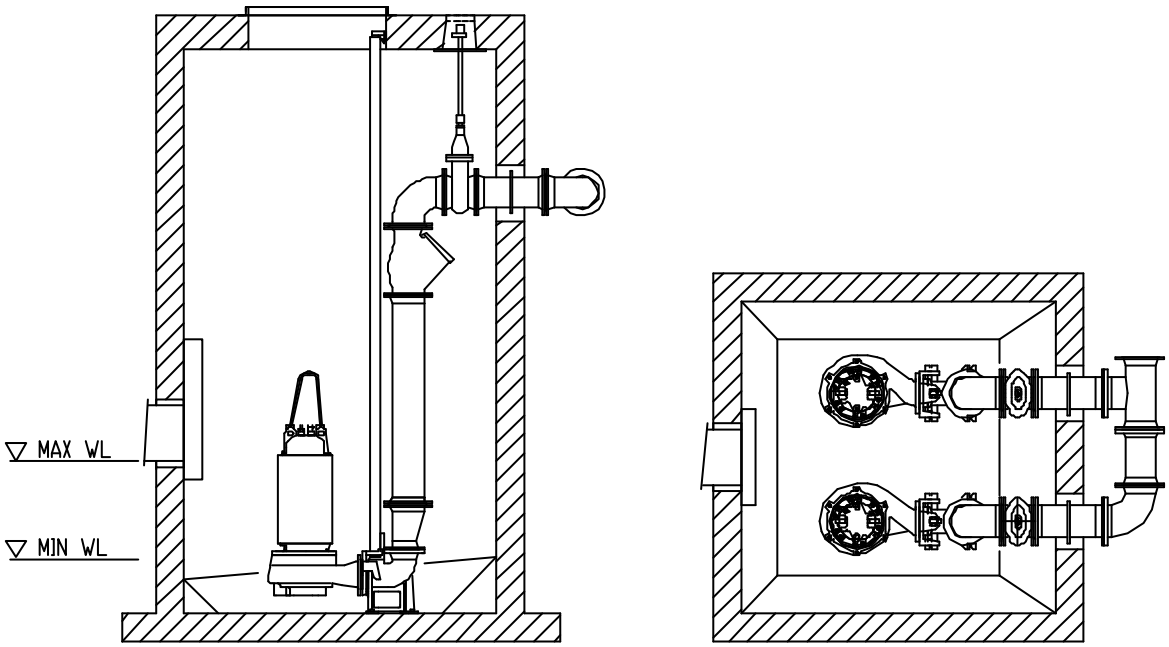

Figure 2: Layout of a standard sewer pumping station

Figure 3 shows a picture of a plunging jet and the area where the entrained air bubbles are present. From the left side the water is dropped from a moderate distance above the water surface. The water depth at which air bubbles are entrained is even larger than the drop distance. If the water in the suction reservoir is in motion, a large quantity of air is likely to be sucked in the pump and transported into the pipeline system.

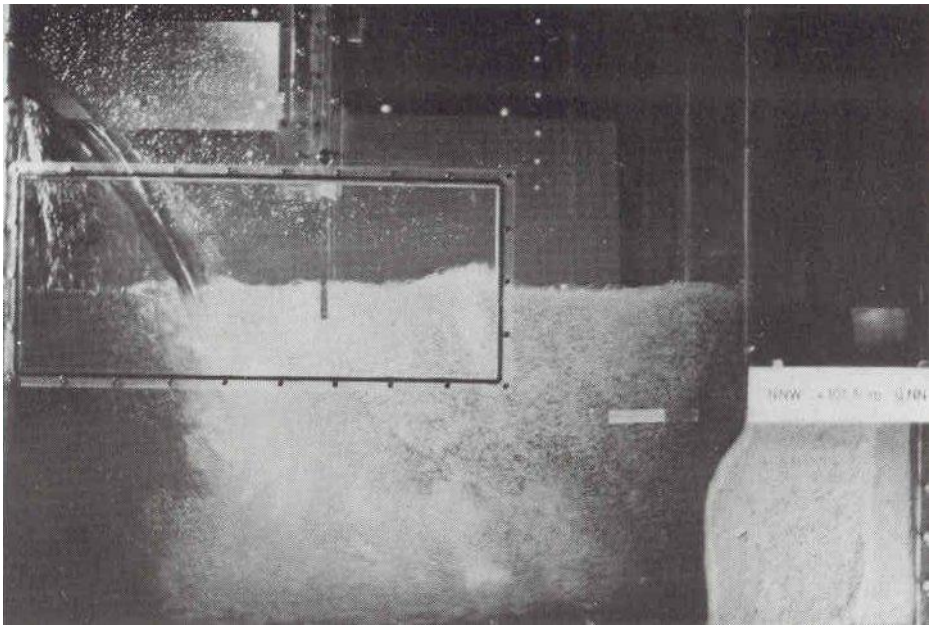

Figure 3: Air entrainment at a plunging jet.

2.2 Check valve

Figure 2 shows a standard layout of a suction reservoir of a wastewater pump station. Check valves are often located in the vertical stand pipe between the pump at the bottom of the suction reservoir and the horizontal transport pipe. When the pump shuts off, the check valve closes. If the check valve is located above the water level of the suction reservoir, the pressure of the water column under the check valve is below atmospheric pressure. Cases are known to have under pressures of 6 m upstream of the check valve. Solved gas can dissolve and form a gas pocket under the check valve. In the worst case the water column can break and a large air volume will be present between the pump and the check valve. The next time the pump restarts, the air or gas pocket is transported further in the system possibly causing capacity reduction.

2.3 Submergence of the pump

Air can be sucked into the pump by air entraining vortices if the water level at the pump's inlet is too low. The critical submergence of the pump depends on inlet velocity, inlet diameter and geometry of the pump and reservoir. If the critical submergence is known, based on e.g. experience or model testing, the appropriate switch-off level can be assessed. However, depending on the system the flow does not stop immediately when the pump is shut off due to inertia of the water in the system.

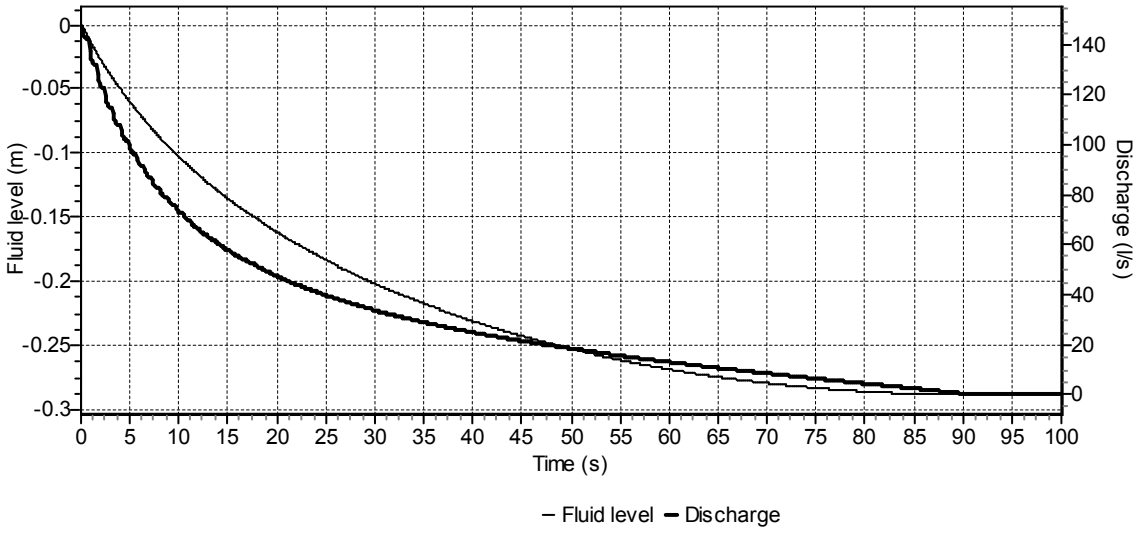

Figure 4: Water level of suction reservoir and subsequent discharge after pump shut-off

To illustrate this subsequent flow that could be delivered after pump shut-off, a simulation is carried out for a simple pipeline system. The system consists of a suction reservoir with 10 m^2, a pump followed by a check valve, 500 m of steel pipe with inner diameter of 300 mm and ends with a reservoir with constant head. At t = 0 seconds the head of both reservoirs are at 0 m and the pump is shut off. **Figure 4** shows the subsequent delivery of water and the resulting water level at the suction reservoir after pump shut-off. The check valve closes after 90 seconds. The total water volume subsequently delivered has been 2.9 m^3. It is assumed that no water is supplied from the sewer. In this example the water level dropped 29 cm after pump shut-off. **Figure 2** left shows a pumping station and its switch-off level (MIN WL). For this pumping station there is a significant possibility that air is entrained in this time interval.

3 EXPERIMENTAL SET-UP

A short experimental loop is built to investigate the behaviour of free gas at high points. The experiments are conducted in a dedicated facility for research on air/gas pockets that are located at the transition from horizontal to inclined pipes. The facility (Figure 5) is specially designed to inject a controlled and monitored airflow into the liquid phase.

From a constant head reservoir a pump circulates water through the experimental facility. A flow control valve (FCV) in combination with an EMF flowmeter and PC adjust the flow rate to its set value. The injection of air into the system results in a head increase of the pump, causing the flow rate to drop. The flow control allows a constant flow rate during head changes.

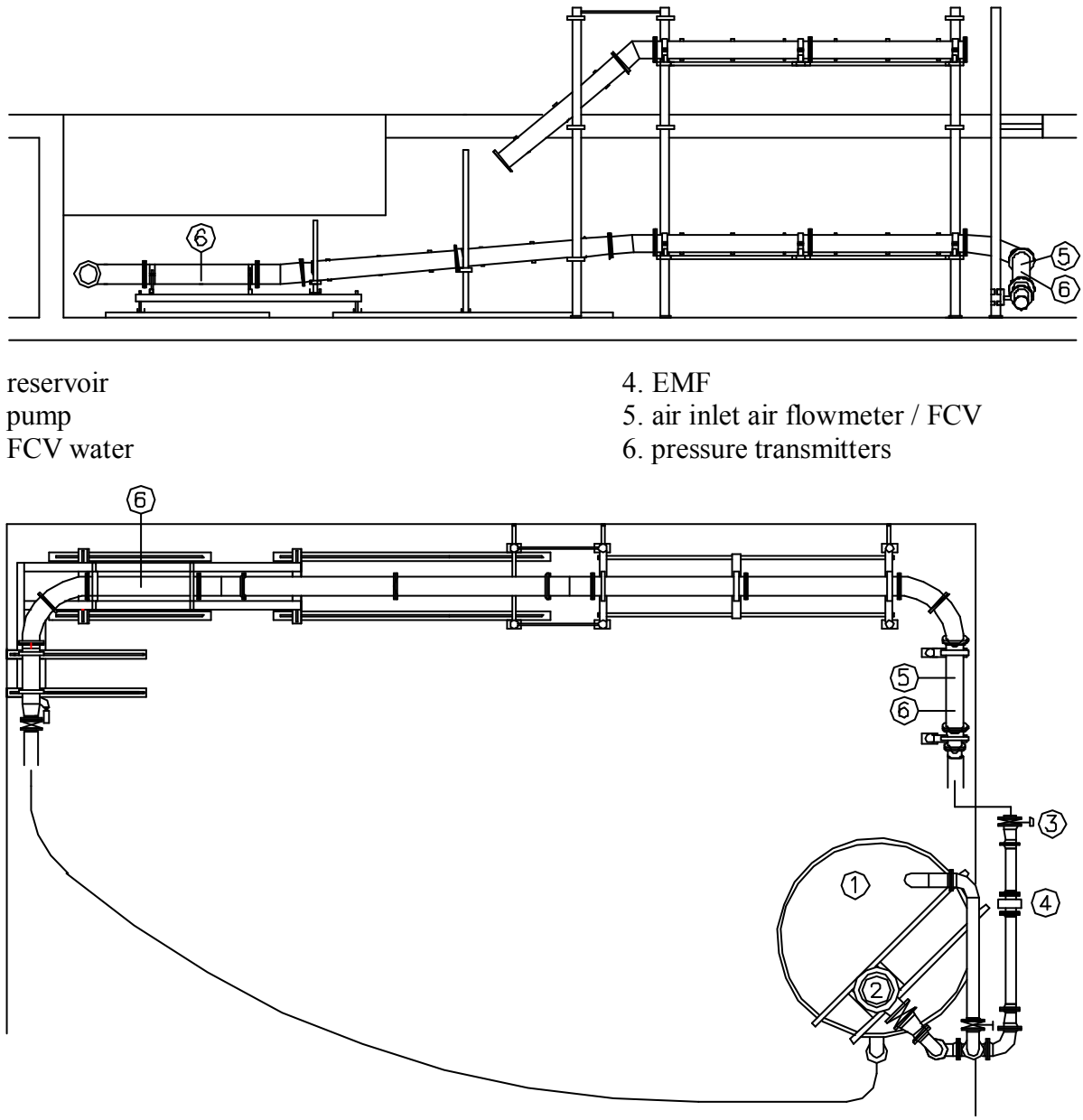

1. reservoir
2. pump
3. FCV water
4. EMF
5. air inlet air flowmeter / FCV
6. pressure transmitters

Figure 5: Top and side view of the experimental set-up.

Air is supplied by the standard 6 bar pressurised air-infrastructure in the building. A combined mass flowmeter and flow control valve adjusts the airflow to its set value. Since the air flowmeter measures mass, the output gives 'nl/min', i.e. a volumetric flow rate at normal conditions (pressure 101325 Pa and temperature 0 °C).

The test section consists of an upward sloped section that incorporates the injection point of the air. This section is followed by a 90 degree mitred bend and a horizontal approach section, a downward sloping section and a horizontal section. This section is made of transparent material (Perspex) with an inner diameter of 220 mm. Flexible hoses connect the test section to the reservoir and pump. The water/air mixture returns to the reservoir over a weir in order to strip as much air as possible from the water.

The facility incorporates the following instrumentation.

	range	uncertainty
EMF DN125	0 – 100 l/s	< 0.25%
Gas flowmeter	1 – 50 nl/min	< 0.5 %
Two absolute pressure transmitters	0 – 3 bara	< 0.1 %
Temperature transmitter	3 to 100 °C	< 0.1 °C

The absolute pressure transmitters are located in the upward inclined section and the downstream horizontal part of the test sections. In order to prevent air from disturbing the pressure measurements, the tapping is located at the bottom of the pipe. The temperature transmitter is located at the reservoir in order to monitor possible temperature increase caused by the pump.
All signals are recorded using an automated data-acquisition system in which the sampling frequency can be adjusted manually ranging between 0 and 10 kHz, the acquired data are stored on a hard disk.

4 TRANSPORT MODES OF AIR/GAS POCKETS

The processes involved in air/gas transport in water are well known and not very complex in themselves:
- Buoyancy
- Drag
- Equilibrium in surface tensions (water/air/wall)

Yet, studying the transport under stationary conditions (constant water and air/gas discharge) reveals that chaotic behaviour occurs. In a downward inclined pipe it is seen that at low concentrations of air/gas the air bubbles stay small (order of magnitude 10 mm), these bubbles have a high drag/buoyancy ratio (Figure 6, left). When either decreasing the water discharge or increasing the air discharge, bubbles show a tendency to aggregate forming larger bubbles having a small drag/buoyancy ratio (Figure 6 right). This leads for larger airflow rates to a chaotic process in which a stream of large air pockets/plugs flows upward (in the opposite directions as the water flow) while a second stream of smaller bubbles is being transported downward (Figure 7).

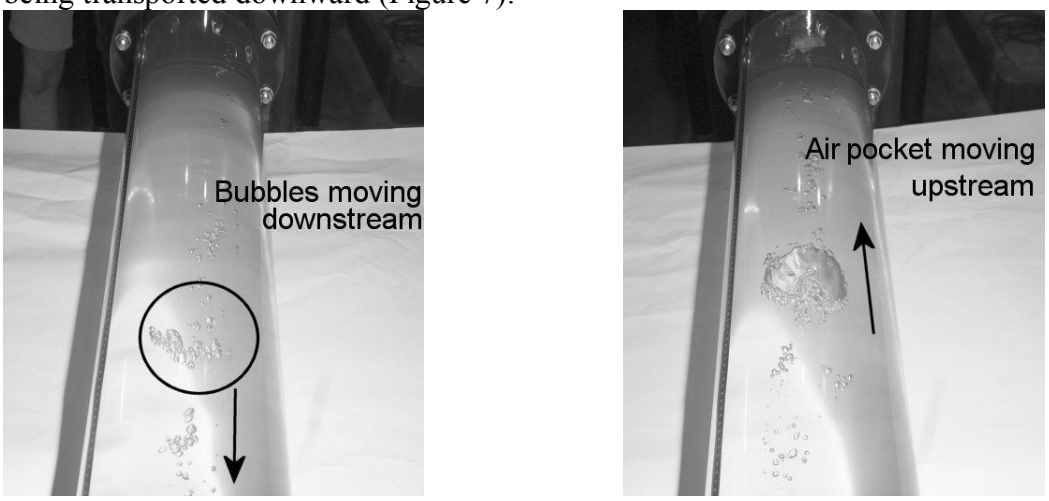

Figure 6: Left: Small bubbles moving downstream, Right: Air pocket moving upstream.

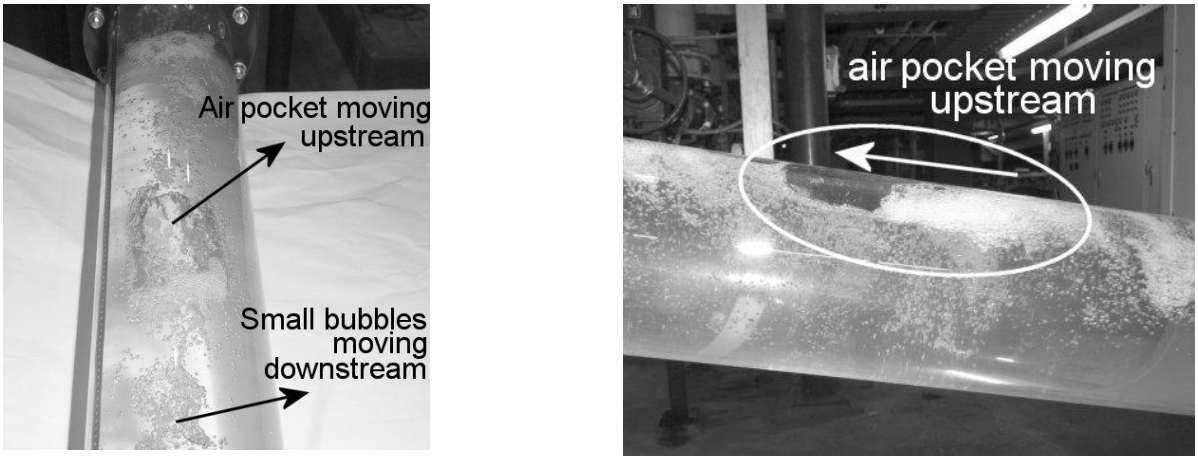

Figure 7: Dual mode flow, large slug moving upstream, small bubbles moving downstream.

Aggregation of air bubbles is a process controlled in part by surface tension and by turbulence; the quantification of this however, will be investigated in more depth in the rest of the research period.
In this 'dual flow mode' much energy is lost since in a given cross section a large percentage of this cross section is air.
Another interesting process is the manner in which air/gas pockets are transported in a downward facing bend.

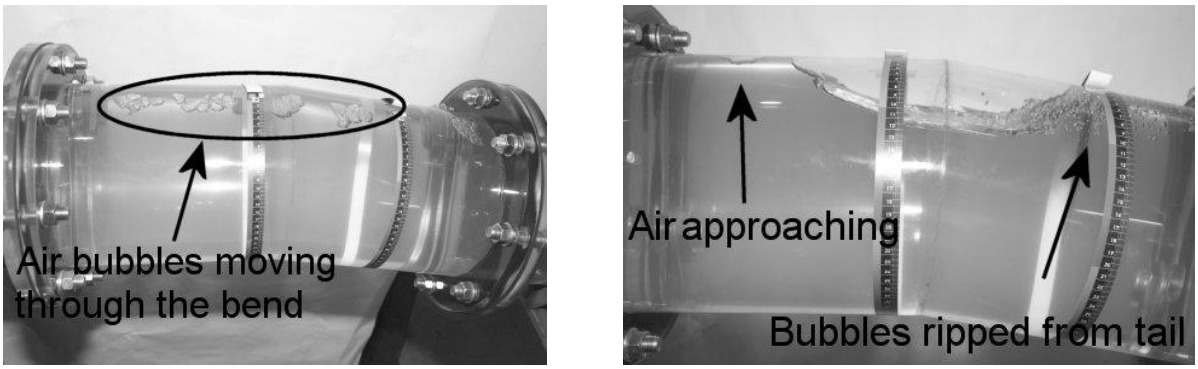

Figure 8: Left shows small air bubbles moving through the bend, Right shows an air pocket acting as buffer.

Small air bubbles are released from the air inlet point. These air bubbles are transported by the water towards the bend. At sufficiently high water velocities, the air bubbles pass the bend unhindered and run down the inclined part (Figure 8 left). In this transport mode air transport is controlled by the drag of the waterflow on the small air bubbles. At the inclined slope the air bubbles may accumulate into larger air pockets that run upstream if their size is large enough, because of their increased buoyancy/drag ratio. This air pocket stretches from upstream of the bend and forms a 'buffer' (Figure 8 right). Now, the small air bubbles introduced at the inlet first merge with the air pocket in the bend. Small air bubbles that are ripped from the tail of the air pocket by turbulence cause air transport from the 'buffer'; the mechanism for air transport is now different. The presence of an air pocket plays a significant role in the transport of air.

5 PRELIMINARY RESULTS

For different slopes (30^o, 20^o, 10^o and 5^o) the head loss between the two pressure transmitters was monitored for a large range of water and air discharges.

The time scale at which the phenomena take place ranges from tenths of seconds to hours. Especially the situations close to the critical velocity and small air discharges show a slow adaptation to changed conditions (e.g. larger flow). Initially, the air discharged from the tail of the 'buffer' may be very close but not equal to the air supply. The air pocket is growing but the grow rate is not visible by eye and can erroneously be taken as stationary.

The upstream and downstream pressures are sampled and the pressure difference is plotted during testing on a large time scale. Figure 9 shows an example of a record of an air pocket growing. Only if the pressure differential line is at a constant level, a measurement is taken.

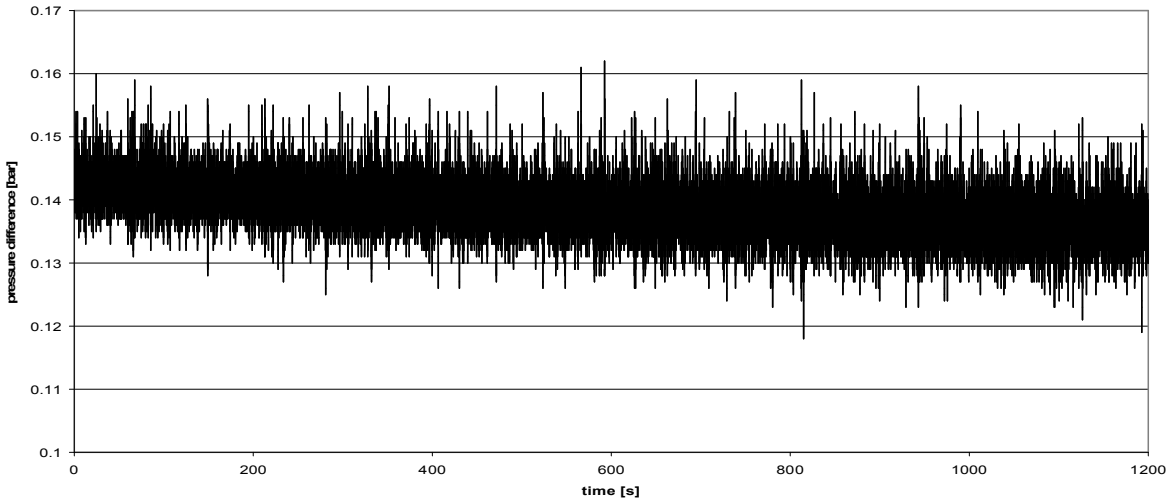

Figure 9: Air pocket growth over a period of 30 minutes

As soon as a stationary situation was achieved, the following signals were recorded; the water and air flow rate, the upstream and downstream pressure and the water temperature. All signals have been recorded for 30 seconds with a sample rate of 100 Hz. The sample rate is sufficiently high to follow the 'spikes' in the pressure difference signal (Figure 10).

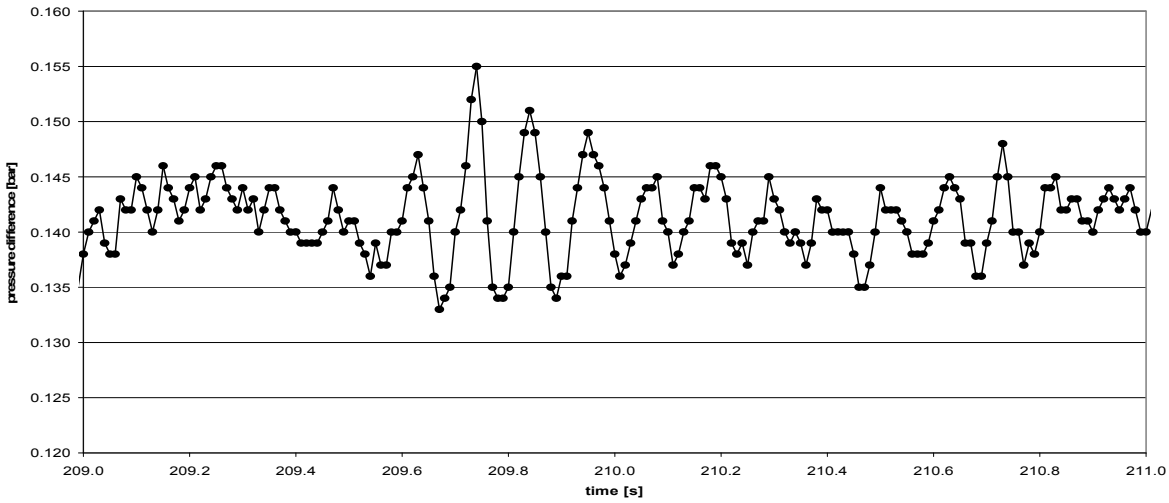

Figure 10: All samples over a period of 2 seconds of a pressure difference time series.

The mean value and standard deviation of the signals are taken per measurement. Further calculations are carried out with the mean values. The energy loss shown in following figures is calculated by subtracting the static head h of the pressure signal p. The total energy loss is defined as:

$$\Delta H_{total} = \frac{(p_1 - p_2)}{\rho g} - (h_1 - h_2),$$

assuming that the velocity head difference between location 1 and 2 is neglected. After measuring the head loss for only water over the flow range (5 to 65 l/s or 0.15 to 1.70 m/s), the lowest flow rate that could discharge the minimum airflow rate (1 nl/min) was determined. If that resulted in a stationary condition, the airflow rate was increased in steps to the maximum flow rate (49 nl/min). It appeared that for all water velocities air is transported. However, at moderate flow velocities, an air pocket is present over the total length of the inclined part of the test section, which results in a maximum head loss.

For larger airflow rates (> 10 nl/min) the results do not show large scatter in the head loss values. After a flow rate change, the flow patterns develop relatively fast to a stationary situation. At the downstream end of the air pocket, small air bubbles move downstream while air plugs (being formed from aggregation of smaller bubbles) move upstream.

For smaller airflow rates (1 to 5 nl/min), the flow patterns may develop very slowly to a stationary situation. Transition times may go up to an hour. It is observed that the flow patterns differ at equal flow rate conditions, depending on the initial state. If small airflow rates are injected in a fully filled pipe a stationary bubble flow condition is yielded without an air pocket (Figure 8 left), resulting in little head loss. If, on the other hand, an air pocket is already formed and the airflow rate is decreased to the same small airflow rate a stationary condition is obtained with an air pocket and thus a larger head loss (Figure 8 right).

Figure 11 shows the measured total head loss for different water flow rates for the 5 ° bend.

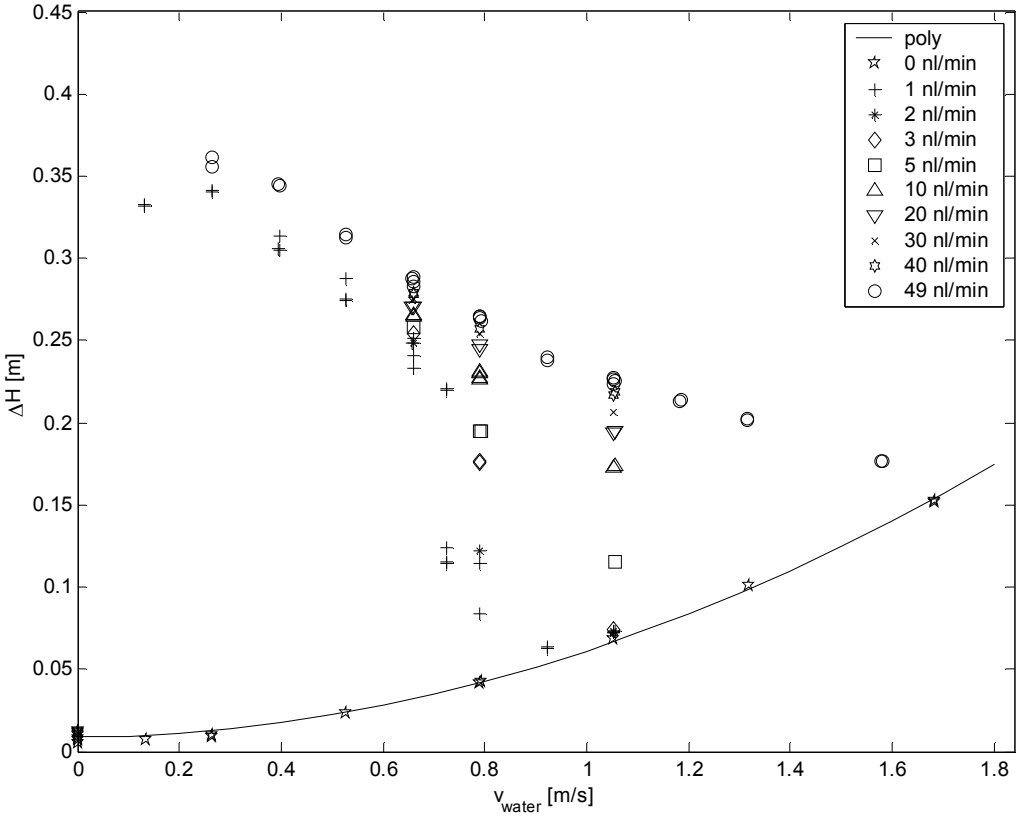

Figure 11: Total head loss as a function of the water flow rate for the 5 ° bend.

For large airflow rates, the head loss line seems to decrease linearly with water flow increase to the head loss values corresponding to the pure water values. For smaller airflow rates, the head loss shows a sudden steeper decrease at 0.75 m/s.

The contribution of the presence of air to the total energy loss is assessed by subtracting the energy loss of the pure water flow (the solid line in Figure 11). The contribution of the air to the energy loss is:

$$\Delta H_{total} = \frac{(p_1 - p_2)}{\rho g} - (h_1 - h_2) - \xi_{geom} \frac{v^2}{2g}$$

in which ξ_{geom} the resistance factor is for the geometry. Figure 12 shows the head loss contribution of the presence of air. For the larger airflow rates, the head loss at constant airflow seems to drop linearly with increasing flow rate. For the lower airflow rates, the head loss line decreases rapidly when the water velocity increases to 0.75 m/s. It should be noted that these lines are for stationary conditions. The adaptation period, i.e. the time it takes for the air pocket to decrease in size, when the water velocity is changed from say 0.7 m/s to 0.8 m/s is in the order of magnitude of 10 minutes.

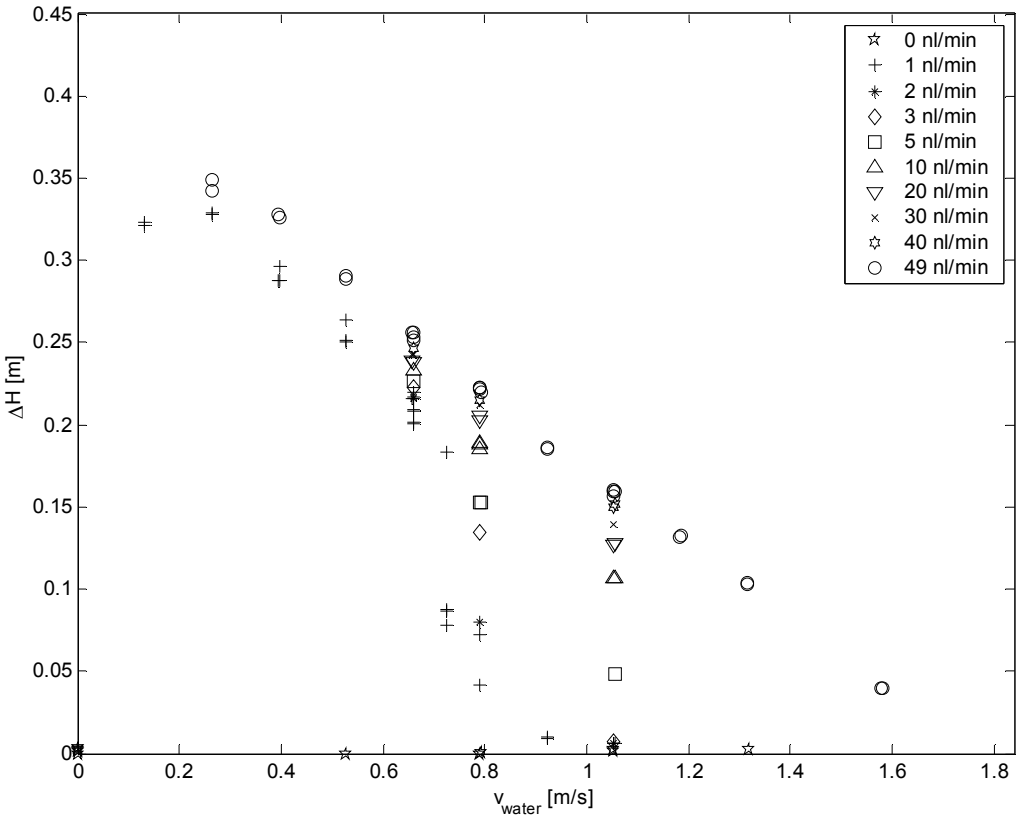

Figure 12: Head loss caused by air for the 5 ° bend.

Additionally to the electronic observations, visual observation has been conducted also. Using markings on the test section, the length and location of the air/water surface have been recorded. By determining the location of the phase transition, the Froude number and specific energy can be assessed. These markings have been added at locations *i* -36, -3, 15 42 72 102 132 162 and 212 cm. The minus sign indicates a location upstream of the bend.

Froude number and specific energy at location *i* are defined as follows:

$$Fr = \frac{v_i}{\sqrt{gD_h}\cos\theta}$$

$$E_i = y_i + \frac{Q_w^2}{2gA_i^2}$$

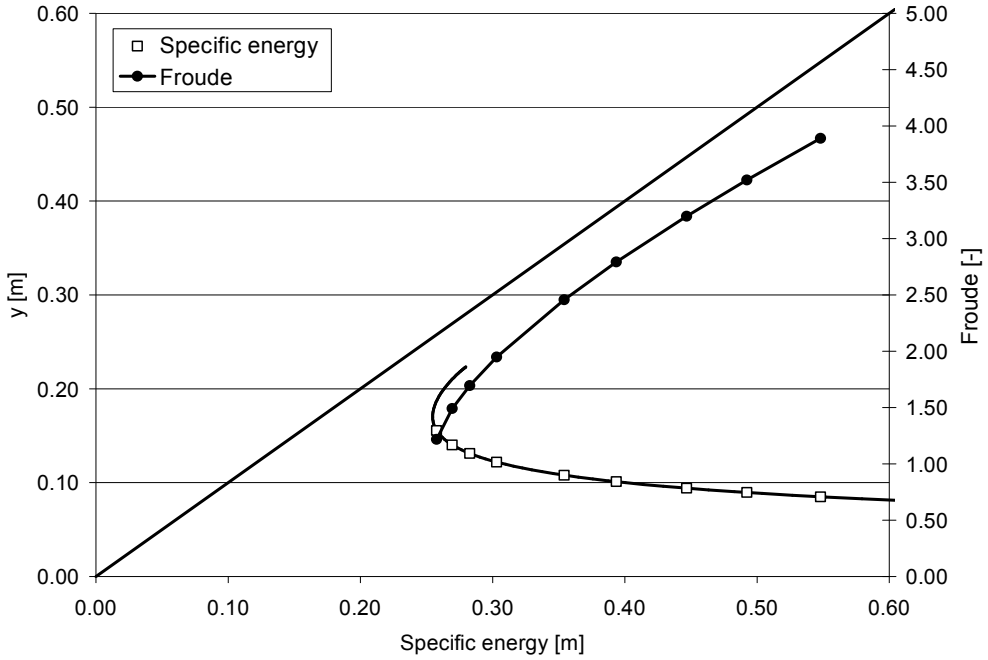

Figure 13: Specific energy curve and Froude for the 10 ° bend

Figure 13 shows the specific energy curve for a water flow rate of 40 l/s for the 10 ° bend, the values measured along the air pocket from location '-34' (most left point) to '212' (most right point) and their corresponding Froude values. Similar to free surface weirs, the free surface flow across the bend tends to go to its minimum energy level corresponding to Froude is 1.

6 DISCUSSION

This paper presents the first results of the study on air pockets in pipelines. Small air bubbles are responsible for the transport of air, while large air plugs flowing against the stream cancel out part of the air discharge at the same time. Regarding velocities that transport air, it showed that lower velocities where found than in the previous studies mentioned (see Figure 1).

Part of the problems due to free gas in pipeline systems is caused by air that is entrained at pumping stations. When designing new pump stations great effort should be put in the prevention of air entrainment. For existing pumping stations that suffer from air entrainment, model tests could provide effective solutions.

If design change is not possible, a sufficiently high water velocity can obtain the removal of gas/air in a system. Another option is to apply air valves at the right location. At the 30° and 20° it is observed that the air pocket was always located at the bend. The flow could not drive it through the bend. For the 10° case, the air could be driven through the bend in the case the air supply was stopped. For the 5° case the air pocket was also located at the inclined part. An air valve at the highest point would be ineffective for pipelines with small inclination. A better understanding of the air pocket behaviour is eminent, when designing the location of the air valves.

Further research will focus on to what extent the open channel flow properties and theory relate to the air pockets in closed conduits.
The mixing zone downstream of the air pocket shows both open channel phenomena such as the flow in a water jump but also closed conduit phenomena such as the plugs moving upstream. Further research will focus on describing these mechanisms that play a role in air transport.

ACKNOWLEDGEMENT

The research is funded by: Foundations RIONED and STOWA, the Waterboards of Aquafin, Brabantse Delta, Delfland, DWR, Fryslân, Municipality of The Hague, Hollandse Eilanden en Waarden, Hollands Noorderkwartier, Reest en Wieden, Rivierenland, Veluwe, Zuiderzeeland and the Engineering/consultancy companies DHV and Grontmij.

REFERENCES

Kamma, P.S. and van Zijl, F.P. (2002) De weerstand in persleidingen voor afvalwater tijdens de gebruiksfase (*The pressure losses of sewer pipeline systems in operation, in Dutch with an English summary)* Rioleringswetenschap- en techniek, jaargang 2 nr- 5, pp. 45-64. ISSN 1568-3788

Kent, J.C. The entrainment of Air by Water Flowing in Circular Conduits with downgrade Slopes. Thesis presented to the University of California, at Berkeley, Calif., in 1952.

Lubbers, C.L. (2003) Capwat: Resultaten van inventarisatie, voortgangsrapportage-02 (Results of the inventory study, part of the Capwat project) H4230.10 Delft Hydraulics.

Walski, T.M. (1994) Hydraulics of corrosive gas pockets in force mains. Water Environment Research, Volume 66, Number 6.

Wisner, P.E. (1975), Removal of air from water lines by hydraulic means, Proceedings of the American Society of Civil Engineers, Journal of the Hydraulics Division, Vol. 83, No. HY2, February, 1975.

Wood, I.R. (1991), Air-entrainment in free-surface flows, AIRH Hydraulic structures design manual 4